Multiple phonon processes contributing to inelastic scattering during thermal boundary conductance at solid interfaces

Patrick E. Hopkins

Citation: J. Appl. Phys. 106, 013528 (2009); doi: 10.1063/1.3169515
View online: http://dx.doi.org/10.1063/1.3169515
View Table of Contents: http://jap.aip.org/resource/1/JAPIAU/v106/i1
Published by the American Institute of Physics.

Multiple phonon processes contributing to inelastic scattering during thermal boundary conductance at solid interfaces

Patrick E. Hopkins[a)]
Engineering Sciences Center, Sandia National Laboratories, P.O. Box 5800, Albuquerque, New Mexico 87185-0346, USA

(Received 20 November 2008; accepted 9 June 2009; published online 15 July 2009)

A new model is developed that accounts for multiple phonon processes on interface transmission between two solids. By considering conservation of energy and phonon population, the decay of a high energy phonon in one material into several lower energy phonons in another material is modeled assuming diffuse scattering. The individual contributions of each of the higher order inelastic phonon processes to thermal boundary conductance are calculated and compared to the elastic contribution. The overall thermal boundary conductance from elastic and inelastic (three or more phonon processes) scattering is calculated and compared to experimental data on five different interfaces. Improvement in value and trend is observed by taking into account multiple phonon inelastic scattering. Three phonon interfacial processes are predicted to dominate the inelastic contribution to thermal boundary conductance. © *2009 American Institute of Physics*.
[DOI: 10.1063/1.3169515]

I. INTRODUCTION

Thermal boundary conductance, or Kapitza conductance,[1] σ_K, is critical in measurement and modeling thermal properties in a wide range of condensed matter nanostructures ranging from carbon nanotubes,[2] to superlattice films[3] and nanowires,[4] to thin metal films.[5–7] As nanostructures are routinely fabricated with critical lengths on the order of carrier mean free paths, the need to understand the fundamental physical processes driving σ_K is increasingly important to interpret and predict thermophysical properties.[8] This is especially significant with the recent results that Fourier's law breaks down even at length scales larger than the mean free in nanostructures,[9] causing σ_K to play a larger role in thermal processes in low dimensional structures. The Kapitza conductance, the inverse of which is the Kaptiza resistance, R_K, creates a temperature drop across the interface that is related to the thermal flux by $\sigma_K=1/R_K=Q_{12}/\Delta T$, where Q_{12} is the heat flux from side 1 to side 2 and ΔT is the interfacial temperature drop.

Several groups have experimentally studied parameters that can affect σ_K, such as substrate damage,[10] quality of crystalline orientation,[11] phonon mean free path,[12] atomic diffusion,[13] and intrinsic vibrational properties of the material (or "acoustic mismatch").[6,7,14] Traditional models for σ_K,[15] however, are rooted in basic assumptions of carrier scattering and fail to capture the experimental values and trends on the parameters discussed above. The most drastic example is reported by Stevens *et al.*,[14] who measured σ_K at room temperature across a wide range of acoustically mismatched interfaces dominated by phonon transport. Their results indicate that the diffuse mismatch model (DMM), the most widely used model to predict phonon interfacial transport,[15] can vary in agreement with the experimental data by over an order of magnitude depending on the acoustic mismatch of the sample. Several physical models have been proposed to explain these discrepancies, including using an exact phonon dispersion in the calculations,[16,17] incorporating electron-phonon resistances at the interface,[18] and accounting for multiple elastic phonon scattering events around the interface.[19,20] All these cases help to explain the discrepancies in the case when the two materials comprising the interface are acoustically matched. However, attempts to explain the deviation between the acoustically mismatched materials and the DMM have resulted in two conflicting theories (electron versus phonon scattering), the origins of which are described below.

Stoner and Maris[21] reported some of the first measurements of σ_K at relatively high temperatures (50–300 K) on a range of acoustically mismatched solid-solid metal/dielectric interfaces. Their results showed that the DMM underpredicted the measured σ_K by over an order of magnitude for interfaces that were heavily mismatched. These surprising results were theoretically explained with analytical studies by Huberman and Overhauser[22] and Sergeev[23,24] via different mechanisms of electron scattering at the metal/dielectric interface. Since the pump-probe thermoreflectance measurement technique employed by Stoner and Maris monitored the electronic response to thermal excitations, this explanation seemed viable until molecular dynamics simulations (MDS) examined the phonon scattering processes affecting σ_K. Using classical MDS, Chen *et al.*[25] and Stevens *et al.*[26] found that σ_K linearly increases with temperature on a variety of acoustically mismatched interfaces. These classical MDS results, which do not take into account quantum effects, such as temperature dependent phonon state filling below the Debye temperature, θ_D, conflict with the predictions of the DMM.

The DMM calculations by Stoner and Maris assumed elastic phonon scattering, that is, a phonon of frequency ω will only transfer energy across an interface by scattering

a)Electronic mail: pehopki@sandia.gov.

with another phonon of frequency ω. Therefore, the temperature dependency of σ_K predictions will be dictated by the phonon population of the lower Debye temperature material. Above the Debye temperature, the phonon population is no longer driven quantum mechanically, but classically,[27] which takes a linear dependence on temperature. Therefore, assuming elastic scattering, σ_K will be constant at temperatures above the Debye temperature of the material with the lower Debye temperature at an interface since σ_K is proportional to the temperature derivative of the phonon population (this will become more clear in Sec. II in the mathematical derivation of the DMM). Since the DMM prediction of constant σ_K in the classical limit is a consequence of assuming elastic phonon scattering at the interface, the linear prediction of σ_K by the aforementioned MDS studies[25,26] suggests that inelastic phonon scattering events could provide additional means of interfacial transport. This could explain the results reported by Stoner and Maris.[21] Recent experimental studies by Hopkins *et al.*[6] and Lyeo and Cahill[7] reported a linear increase in σ_K with temperature on a wide range of acoustically mismatched interfaces, supporting the inelastic scattering theory. These experimental studies suggested that the inelastic scattering channel of σ_K could be driven by three (or more) phonon processes at the interface, paralleling the familiar Klemens process between a high energy optical phonon and several lower energy acoustic phonons.[28]

Although the MDS and experimental studies support the assumption that inelastic phonon scattering participates in σ_K, there are no analytical models for σ_K that specifically take into account the multiple phonon processes in interface transmission, thereby physically modeling the effects of inelastic scattering on σ_K. Chen[29] and Dames and Chen[30] developed expressions for phonon transmission that accounts for inelastic scattering based on the total internal energy of each phonon system on either side of the interface; these expressions assume phonons of all energies on both sides of the interface are participating in σ_K, which does not consider the specific allowed phonon scattering events governed by energy conservation. Hopkins and Norris[31] developed a new model, the joint frequency diffuse mismatch model (JFDMM), that accounts for inelastic scattering by changing the density of states of the phonon flux approaching the interface; again, this model does not specifically examine phonon scattering and conservation during energy transmission. Multiharmonic processes on phonon transmission in a two dimensional transition layer near the interface were considered by Kosevich;[32] this theory, similar to the JFDMM, assumes that the transition layer allows for vibrational modes around the interface that are not allowed in one of the materials (essentially inelastic scattering), but does not consider phonon scattering or quantum effects in phonon transmission. In another model, Hopkins and Norris[33] separated elastic and inelastic scattering contributions, but their transmission models required experimental data of σ_K as a function of temperature. Obviously, there is a great need for an analytical model for σ_K that accounts for the multiple phonon processes and examines the fundamental phonon physics contributing to inelastic scattering.

In this paper, a new model for phonon transmission is developed that takes into account multiple phonon scattering events between two materials by considering energy conservation in individual phonon scattering events. This model provides a much more physical development of the effects of inelastic scattering on σ_K than previous models that account for inelastic scattering. The model developed in this paper in addition to the evidence in the experimental and MDS trends will give a clear picture of how inelastic phonon scattering contributes to σ_K, and will further support the theory that inelastic phonon scattering adds an additional channel to σ_K instead of electron-interface scattering processes.

The model developed in this work makes three basic assumptions: (1) each solid adjacent to the interface can be described with an isotropic Debye dispersion; (2) phonon scattering at the interface is diffuse, that is, the scattered mode loses all memory of polarization and incident angle simplifying the problem to essentially just a conservation of energy consideration; and (3) the material designated as side 1 has a smaller vibrational spectra and lower speed of sound than the material designated as side 2 (i.e., side 1 is the "softer" material and side 2 is the "stiffer" material). The consequences and potential error associated with these assumptions will be addressed in Sec. II. In addition, Sec. II will present the derivation of the DMM and analyze the consequences of assuming elastic phonon scattering. Section III will walk through the development of the inelastic scattering transmission coefficients, and compare this inelastic scattering transmission model to previous models for elastic and inelastic phonon scattering. Finally, Sec. IV will compare thermal boundary conductance calculations using the models for elastic and inelastic transmission coefficients to experimental data. This new model that takes into account inelastic scattering by considering multiple phonon processes in interface transmission shows excellent agreement with experimental data on acoustically mismatched samples where inelastic scattering was previously only *assumed* to dominate σ_K.

II. THE DMM AND ELASTIC SCATTERING

Thermal boundary conductance calculations begin by considering an incident flux of phonons impinging on an interface. Using the equation of phonon radiative transfer, the phonon heat flux can be calculated by

$$Q_1 = \sum_j \int_{\Omega=4\pi} \int_{\omega_{c,1,j}} \mu I_{1,j}(z,t,\omega,v,\Omega) d\omega d\Omega, \tag{1}$$

where μ is the cosine of the angle between the phonon propagation direction and the z-direction (θ), Ω is the solid angle, I is the directional spectral intensity of phonons per unit area, z and t are the position and time of the phonons, respectively, ω is the phonon frequency, ω_c is the cutoff frequency, and j represents the phonon polarization in which I is summed over all polarization modes. To account for the heat flux across the interface, Eq. (1) is multiplied by a phonon transmission coefficient, $\alpha(z,t,\omega,v,\theta)$, and related to σ_K via

$$\sigma_K = \frac{\partial}{\partial T}\left[\sum_j \int_{\Omega=4\pi}\int_{\omega_{c,1,j}}\int_{\theta} \mu I_{1,j}(z,t,\omega,v,\Omega)\alpha_{12} \times(z,t,\omega,v,\theta)d\theta d\omega d\Omega\right]. \quad (2)$$

As stated in Sec. II, the analysis in this paper will assume that phonons are scattered diffusely. Since this paper focuses on the effects of inelastic scattering on σ_K, a phenomenon that is observed at relatively high temperatures in experimental studies, this diffuse scattering assumption is valid due to the thermal wavelength of the phonon system at these temperatures compared to characteristic scattering scales at the interface. The representative wavelength of the phonon flux approaching the interface can be estimated by the thermal coherence length, L, which can be thought of the spatial extent of the phonon wavepacket.[34] The coherence length for each phonon polarization, given by $L_j = hv_j/k_BT$, where h is Planck's constant, v is the phonon velocity, and k_B is Boltzmann's constant, is related to the degree of specularity of the phonon scattering event via[35]

$$p = \exp\left[-\frac{16\pi^2\delta_{\text{rms}}^2}{L_j}\right], \quad (3)$$

where p is the specularity parameter, which estimates the probability that phonons are specularly scattered, and δ_{rms} is the asperity parameter of the interface (mean square deviation of the height of the surface from the reference plane). It is apparent that as the product $\delta_{\text{rms}}T$ increases, the probability of diffuse scattering increases. Also, as the velocity of the phonons in a crystal increases, the probability of diffuse scattering decreases. As previously mentioned, evidence of inelastic scattering has been reported at relatively high temperatures ($T > 50$ K). Diamond, having one of the highest phonon velocities of any pure materials (longitudinal velocity of 17 500 m s^{-1}),[36] would therefore be the most likely to experience specular phonon scattering at an interface. Consider diamond phonons approaching an interface at 50 K with only 1 ML (monolayer) of roughness (lattice constant of diamond is approximately 0.357 nm).[27] Using Eq. (3), phonons have less than a 3.5% probability of scattering specularly, with the probability decreasing to 0.1% by 100 K. Therefore, for material systems and temperatures of interest in this work, diffuse phonon scattering is a valid assumption.

By assuming diffuse phonon scattering at the interface, the transmission coefficient in Eq. (2) can be estimated under equilibrium conditions. First, since diffuse scattering means that the scattered phonon has no memory of the mode or frequency from which it originated before the scattering event, the transmitted phonon flux and transmission coefficient are no longer directionally dependent, and can therefore be estimated as isotropic, so Eq. (2) becomes

$$\sigma_K = \frac{\partial}{\partial T}\left[\sum_j \int_{\omega_{c,1,j}} \pi I_{1,j}(\omega,v,T)\alpha_{12}(\omega,T)d\omega\right], \quad (4)$$

where $I_{1,j}(z,t,\omega,v,\Omega)$ has been replaced with the expression for the isotropic equilibrium intensity, $I_{1,j}(\omega,v,T)$, at the equivalent interface temperature. Since the interface scatters phonons diffusely, the interface can be treated as a completely thermalizing (black) boundary, so the intensity can be described as $I_{1,j}(\omega,v,T) = \hbar\omega v_j N_j(\omega,T)/4\pi$, where $\hbar$ is modified Planck's constant and $N_j(\omega,T)$ is the number of phonons at a given frequency, temperature, and polarization per unit volume. $N_j(\omega,T)$ can be calculated by $N_j(\omega,T) = g_j(\omega)f_0(\omega,T)$, where $g_j(\omega)$ is the phonon density of states and $f_0(\omega,T)$ is the Bose–Einstein distribution function. In essence, Eq. (4) is the DMM in its most general form.

Recognizing that, by the nature of diffuse scattering, $\alpha_{12}(\omega,T) + r_{12}(\omega,T) = 1$ and $r_{12}(\omega,T) = \alpha_{21}(\omega,T)$, where $r_{12}(\omega,T)$ is the phonon reflection coefficient, then reciprocity requires that $\alpha_{21}(\omega,T) = 1 - \alpha_{12}(\omega,T)$. Applying detailed balance on the phonon flux approaching the interface in each material yields

$$\sum_j \int_{\omega_{c,1,j}} \hbar\omega v_{1,j} g_{1,j}(\omega) f_0(\omega,T)\alpha_{12}(\omega,T)d\omega = \sum_j \int_{\omega_{c,2,j}} \hbar\omega v_{2,j} g_{2,j}(\omega) f_0(\omega,T)[1-\alpha_{12}(\omega,T)]d\omega. \quad (5)$$

Note that in Eq. (5), the transmission coefficient is a function of the phonon frequency, and the integrations are prescribed over the entire phonon spectrum in each material. At this point, to calculate the transmission coefficient, assumptions about energy conservation and the phonon scattering mechanisms at the interface must be made.

Assuming elastic scattering, since one phonon can only transfer energy to one other phonon with the same energy, no phonons with frequencies above $\omega_{c,1}$ can participate in σ_K, so Eq. (5) becomes

$$\alpha_{12}^{(2)} = \frac{\sum_j v_{2,j} g_{2,j}(\omega)}{\sum_j v_{1,j} g_{1,j}(\omega) + \sum_j v_{2,j} g_{2,j}(\omega)}, \quad (6)$$

where the superscript (2) denotes that only two phonons are participating in this scattering event, and hence this is the elastic transmission coefficient. Assuming a Debye density of states, that is, $g_j(\omega) = \omega^2/2\pi^2 v_j^3$, Eq. (6) reduces to the familiar elastic transmission coefficient often associated with the DMM, given by

$$\alpha_{12}^{(2)} = \frac{\sum_j v_{2,j}^{-2}}{\left(\sum_j v_{1,j}^{-2} + \sum_j v_{2,j}^{-2}\right)}. \quad (7)$$

Examining the opposite limit, assuming that all phonons of all frequencies in each material will transmit energy across the interface, Eq. (5) can be rewritten to determine the transmission coefficient as

$$\alpha_{12}(T) = \frac{\sum_j \int_{\omega_{c,2,j}} \hbar\omega v_{2,j} g_{2,j}(\omega) f_0(\omega,T) d\omega}{\sum_j \int_{\omega_{c,1,j}} \hbar\omega v_{1,j} g_{1,j}(\omega) f_0(\omega,T) d\omega + \sum_j \int_{\omega_{c,2,j}} \hbar\omega v_{2,j} g_{2,j}(\omega) f_0(\omega,T) d\omega}, \quad (8)$$

which, assuming a constant phonon velocity across the entire Brillouin zone (i.e., Debye), Eq. (8) is rewritten into the form similar to that derived by Chen[29] and Dames and Chen[30] given by

$$\alpha_{12}(T) = \frac{\sum_j v_{2,j} U_{2,j}(T)}{\sum_j v_{1,j} U_{1,j}(T) + \sum_j v_{2,j} U_{2,j}(T)}, \quad (9)$$

where U is the internal energy of the phonon system. Note in this transmission coefficient derivation, energy conservation in individual scattering events is not considered since the entire phonon population in a given side is governed by one transmission probability at a given temperature. This development does not specifically consider the energy conserving processes of a high frequency phonon in side 2 breaking down into several lower frequency phonons in side 1, which is the fundamental multiple phonon interfacial process contributing to inelastic scattering during σ_K.

Assuming a Debye dispersion gives rise to Eqs. (7) and (9) and makes transmission a trivial calculation when assuming elastic scattering. The Debye assumption has its limitations, especially in relatively high temperature studies where phonons are excited close to the zone boundary and the change in ω is no longer linear with the change in wavevector, $\vec{q}$. In this case, the phonon group velocity is no longer constant and varies with ω, and the density of states no longer takes the compact Debye form. Therefore, since the phonon group velocity vanishes at the zone edge, the Debye assumption should cause an overestimate in σ_K. In fact, using a real dispersion in transmission and σ_K calculations makes the predictions of σ_K larger at lower temperatures ($T < \theta_D$), reach a constant value at temperatures lower than the Debye predictions, and predict a slightly lower σ_K in the classical limit.[17] Experimental data clearly dominated by inelastic scattering are in temperature regimes where a Debye approximation predicts a constant σ_K; therefore, the use of the real dispersion would give the same trend. In heavily acoustically mismatched samples (e.g., Pb/diamond and Bi/diamond), the DMM predictions are almost an order of magnitude less than the experimental data, so the slight change due to using a real dispersion will not affect the results. In addition, for a range of acoustically mismatched samples that will be analyzed in this work (Pb/diamond, Bi/diamond, Au/diamond, and Pt/AlN), using the Debye model with elastic scattering assumptions has shown to give a reliable estimation of the contribution of elastic scattering to σ_K.[33] Therefore, the specific results and calculations in Secs. III and IV will use assume a Debye dispersion. This allows the cutoff frequency can be calculated by $\omega_{c,1,j} = v_{1,j}(6\pi^2 N_1)^{1/3}$, where N_1 is the total number of oscillators per until volume of side 1.[27] In cubic structures (such as metal with one atom per unit cell), N_1 is simply the atomic density, calculated by $N_1 = \rho N_A / M$, where ρ is the mass density, N_A is Avogadro's number, and M is the atomic weight. However, in structures with more than one atom per unit cell (for example, diamond structures with diatomic basis such as Si or diamond), the number of primitive cells per unit volume must be divided by the number of atoms in the basis.[30] Therefore, for a diatomic basis, $N_1 = \rho N_A / 2M$.

III. INELASTIC SCATTERING AND INTERFACIAL TRANSMISSON

Consider Eq. (5), which exploits detailed balance on the phonon flux at the interface in the event of diffuse scattering. Taking into account energy conservation in multiple phonon processes, or an n phonon process where n is any integer, then a phonon of frequency $(n-1)\omega$ can break down into $n-1$ phonons of frequency ω. An example of a three phonon process is then modeled as a phonon of frequency 2ω breaking down into two phonons of frequency ω. (Note that a more general three phonon processes could be described as a phonon of frequency ω_1 breaking down into two phonons of frequencies ω_2 and ω_3, where $\omega_1 = \omega_2 + \omega_3$; however, in an effort to develop a closed form analytical model to describe this anharmonic process, only the process of a high frequency phonon breaking down into two equal low frequency phonons will be discussed since the $\omega_1 = \omega_2 + \omega_3$ situation would involved detailed probabilistic simulations and would not result in the closed form model that is sought in this work.) Detailed balance is then invoked on all three phonon process at the interface, which gives

$$\sum_j 2(\hbar\omega) v_{1,j} [g_{1,j}(\omega)] f_0(\omega,T) \alpha_{12}^{(3)}(\omega,T) = \sum_j \hbar(2\omega) v_{2,j} g_{2,j}(2\omega) f_0(2\omega,T)[1 - \alpha_{12}^{(3)}(\omega,T)], \quad (10)$$

where the superscript (3) on $\alpha_{12}^{(3)}(\omega,T)$ refers to the number of phonons participating in interface transmission. Equation (10) can be simplified with a Debye assumption, yielding

$$\sum_j 2\hbar\omega \frac{\omega^2}{2\pi^2 v_{1,j}^2} \frac{1}{\exp\left[\frac{\hbar\omega}{k_B T}\right]-1} \alpha_{12}^{(3)}(\omega,T) = \sum_j 2\hbar\omega \frac{4\omega^2}{2\pi^2 v_{2,j}^2} \frac{1}{\exp\left[\frac{2\hbar\omega}{k_B T}\right]-1} [1-\alpha_{12}^{(3)}(\omega,T)]. \tag{11}$$

So that the transmission coefficient for a phonon of frequency ω undergoing a three phonon, energy conserving, scattering process at the interface is given by

$$\alpha_{12}^{(3)}(\omega,T) = \frac{\sum_j \frac{4}{v_{2,j}^2\left(\exp\left[\frac{2\hbar\omega}{k_B T}\right]-1\right)}}{\sum_j \frac{1}{v_{1,j}^2\left(\exp\left[\frac{\hbar\omega}{k_B T}\right]-1\right)} + \sum_j \frac{4}{v_{2,j}^2\left(\exp\left[\frac{2\hbar\omega}{k_B T}\right]-1\right)}}, \tag{12}$$

where Eq. (12) can now be used in Eq. (4) to determine σ_K in the event that only three phonon processes are contributing to interfacial transport. Since Eq. (12) represents a transmission probability assuming all phonons are undergoing three phonon processes, this ignores the effect of elastic scattering. Assuming a perfect interface where phonons only undergo one scattering event, they can either lose energy by scattering with one phonon of the same energy (elastic), or through a three phonon process (inelastic), or four phonon process (inelastic), etc. Therefore, although Eq. (12) considers the three phonon process, it does not account for phonons that have already been scattered via elastic processes. The number of phonons that have undergone elastic processes in side 1 and side 2 are $\alpha_{12}^{(2)} g_j(\omega) f_0(\omega,T)$ and $[1-\alpha_{12}^{(2)}] g_j(\omega) f_0(\omega,T)$, respectively, where $\alpha_{12}^{(2)}$ is the elastic transmission coefficient (two phonons) given by Eq. (7). Therefore, detailed balance on the remaining phonons undergoing three phonon scattering yields

$$2(\hbar\omega) v_{1,j}[g_{1,j}(\omega)] f_0(\omega,T)[1-\alpha_{12}^{(2)}]\alpha_{12,j}^{(3)}(\omega,T) = \hbar(2\omega) v_{2,j} g_{2,j}(2\omega) f_0(2\omega,T)\alpha_{12}^{(2)}[1-\alpha_{12}^{(3)}(\omega,T)], \tag{13}$$

when $0<\omega\leq\omega_{c,1,j}/2$ and

$$2(\hbar\omega) v_{1,j}[g_{1,j}(\omega)] f_0(\omega,T)[1-\alpha_{12}^{(2)}]\alpha_{12,j}^{(3)}(\omega,T) = \hbar(2\omega) v_{2,j} g_{2,j}(2\omega) f_0(2\omega,T)[1-\alpha_{12,j}^{(3)}(\omega,T)], \tag{14}$$

when $\omega_{c,1,j}/2<\omega\leq\omega_{c,1,j}$. Note that now the three phonon transmission coefficient is mode dependent due to the number of conservation since the longitudinal and transverse branches have different cutoff frequencies. With the Debye assumption, Eqs. (13) and (14) yield a three phonon transmission coefficient of

$$\alpha_{12,j}^{(3)}(\omega,T) = \frac{\frac{4\alpha_{12}^{(2)}}{v_{2,j}^2\left(\exp\left[\frac{2\hbar\omega}{k_B T}\right]-1\right)}}{\frac{[1-\alpha_{12}^{(2)}]}{v_{1,j}^2\left(\exp\left[\frac{\hbar\omega}{k_B T}\right]-1\right)} + \frac{4\alpha_{12}^{(2)}}{v_{2,j}^2\left(\exp\left[\frac{2\hbar\omega}{k_B T}\right]-1\right)}}, \tag{15}$$

when $0<\omega\leq\omega_{c,1,j}/2$ and

$$\alpha_{12,j}^{(3)}(\omega,T) = \frac{\frac{4}{v_{2,j}^2\left(\exp\left[\frac{2\hbar\omega}{k_B T}\right]-1\right)}}{\frac{[1-\alpha_{12}^{(2)}]}{v_{1,j}^2\left(\exp\left[\frac{\hbar\omega}{k_B T}\right]-1\right)} + \frac{4}{v_{2,j}^2\left(\exp\left[\frac{2\hbar\omega}{k_B T}\right]-1\right)}}, \tag{16}$$

when $\omega_{c,1,j}/2<\omega\leq\omega_{c,1,j}$. This approach assumes that elastic scattering is more probable than three phonon scattering, which is more probably than four phonon scattering, etc. This is true for anharmonic decay of optical phonons.[37] Therefore, for any n phonon process, the transmission coefficient will be separated into $n-1$ intervals due to phonon conservation to take into account the more probable $n-1$ phonon scattering processes. For any n phonon inelastic process ($n>2$), the transmission coefficient is defined as

$$\alpha_{12,j}^{(n)}(\omega,T)=\frac{(n-1)^2\prod_{x=0}^{n-3}\alpha_{12}^{(x+2)}\Big/\upsilon_{2,j}^2\left(\exp\left[\frac{(n-1)\hbar\omega}{k_BT}\right]-1\right)}{\prod_{x=0}^{n-3}[1-\alpha_{12}^{(x+2)}]\Big/\upsilon_{1,j}^2\left(\exp\left[\frac{\hbar\omega}{k_BT}\right]-1\right)+(n-1)^2\prod_{x=0}^{n-3}\alpha_{12}^{(x+2)}\Big/\upsilon_{2,j}^2\left(\exp\left[\frac{(n-1)\hbar\omega}{k_BT}\right]-1\right)},\quad 0<\omega<\frac{\omega_{c,j}}{(n-1)},$$

$$\alpha_{12,j}^{(n)}(\omega,T)=\frac{(n-1)^2\prod_{x=1}^{n-3}\alpha_{12}^{(x+2)}\Big/\upsilon_{2,j}^2\left(\exp\left[\frac{(n-1)\hbar\omega}{k_BT}\right]-1\right)}{\prod_{x=0}^{n-3}[1-\alpha_{12}^{(x+2)}]\Big/\upsilon_{1,j}^2\left(\exp\left[\frac{\hbar\omega}{k_BT}\right]-1\right)+(n-1)^2\prod_{x=1}^{n-3}\alpha_{12}^{(x+2)}\Big/\upsilon_{2,j}^2\left(\exp\left[\frac{(n-1)\hbar\omega}{k_BT}\right]-1\right)},\quad \frac{\omega_{c,j}}{(n-1)}<\omega<\frac{2\omega_{c,j}}{(n-1)},$$

$$\vdots$$

$$\alpha_{12,j}^{n}(\omega,T)=\frac{(n-1)^2\Big/\upsilon_{2,j}^2\left(\exp\left[\frac{(n-1)\hbar\omega}{k_BT}\right]-1\right)}{\prod_{x=0}^{n-3}[1-\alpha_{12}^{(x+2)}]\Big/\upsilon_{1,j}^2\left(\exp\left[\frac{\hbar\omega}{k_BT}\right]-1\right)+(n-1)^2\Big/\upsilon_{2,j}^2\left(\exp\left[\frac{(n-1)\hbar\omega}{k_BT}\right]-1\right)},\quad \frac{(n-2)\omega_{c,j}}{(n-1)}<\omega<\omega_{c,j},\tag{17}$$

where $n_{\max}$ the maximum n for an interface, that is, the maximum number of phonons that a high frequency side 2 phonon can break down into by scattering and transmitting energy to side 1 phonons, which can be estimated by $n_{\max}=\text{floor}(\omega_{c,2,j}/\omega_{c,1,j})+1$, where "floor" is the floor function. Figure 1 shows the longitudinal and transverse three and four phonon transmission coefficients as a function of frequency at 100 and 300 K for Pb/diamond. These values are normalized by the elastic transmission coefficient, $\alpha_{12}^{(2)}$. Pb/diamond shows evidence of inelastic scattering,[6,7] and its Debye temperature ratio, which quantifies the acoustic mismatch of the interface, is 0.047. Note that by the estimation for $n_{\max}$, the longitudinal and transverse branches of Pb/diamond can theoretically participate in 11 and 19 phonon processes, respectively. As seen in Fig. 1, three phonon processes, $\alpha_{12}^{(3)}$, do not contribute significantly to energy transfer processes at low frequencies ($\omega\leq\omega_{c,1,j}/2$), showing less than 4% of $\alpha_{12}^{(2)}$ in the longitudinal transmission and about 1% of $\alpha_{12}^{(2)}$ in the transverse transmission. However, above $\omega_{c,1,j}/2$, where the side 2 phonons participating in the three phonon processes have not already elastically scattered, the transmission probability increases to that of or above $\alpha_{12}^{(2)}$. The transmission increases as the temperature increases due to more phonons in side 2 (diamond) being able to participate in energy transmission and three phonon processes. Similar trends in frequency and temperature are predicted in $\alpha_{12}^{(4)}$: negligible transmission when $\omega\leq\omega_{c,1,j}/3$, an increase in transmission when $\omega_{c,1,j}/3\leq 2\omega_{c,1,j}/3$ which is still less than $\alpha_{12}^{(3)}$, and then when $2\omega_{c,1,j}/3\leq\omega_{c,1,j}$, the predicted $\alpha_{12}^{(4)}$ transmission is greater than both $\alpha_{12}^{(2)}$ and $\alpha_{12}^{(3)}$. Similar trends continue with higher order phonon processes (i.e., 5, 6, and n phonon processes). Section IV will consider the effects of these transmission processes on σ_K.

IV. MODELING INELASTIC SCATTERING IN THERMAL BOUNDARY CONDUCTANCE

Since the elastic and inelastic channels of σ_K can be modeled as parallel resistors,[26,33] the elastic and inelastic portions of the phonon intensity, I, are additive. Since I across the interface is simply the transmission coefficient multiplied by I, then the total transmission during elastic and n phonon inelastic processes is simply $\alpha_{12}(\omega,T)=\Sigma_{n=2}^{n_{\max}}\alpha_{12}^{(n)}$

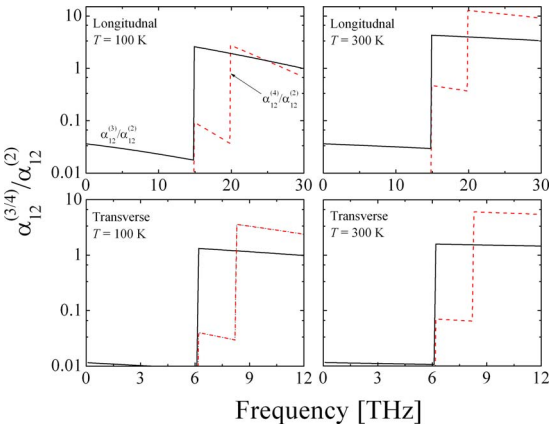

FIG. 1. (Color online) Three and four phonon transmission probabilities for Pb/diamond interfaces using Eq. (17). The data are normalized by the elastic scattering transmission probability, $\alpha_{12}^{(2)}$, given in Eq. (7). The contributions of the multiphonon processes to energy transmission increases with temperature even though the temperatures in the calculations are above the Debye temperature of Pb (~100 K) (Ref. 27) since the diamond phonon population is changing based on the Bose–Einstein distribution below the Debye temperature (Debye temperature of diamond ~2230 K) (Ref. 27). Also, note that higher frequency Pb phonons contribute more to higher order phonon processes since higher frequency diamond phonons are required as the order of the phonon process increases.

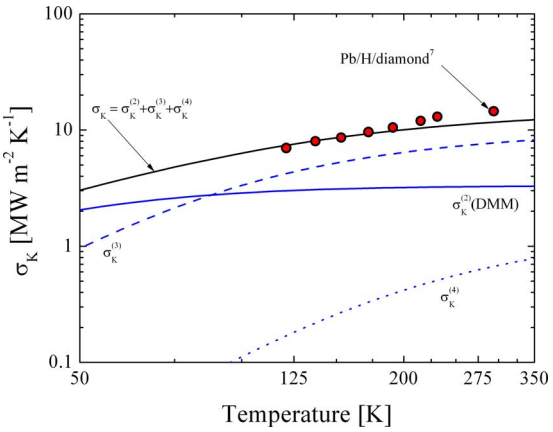

FIG. 2. (Color online) The total predicted thermal boundary conductance, $\sigma_K=\sigma_K^{(2)}+\sigma_K^{(3)}+\sigma_K^{(4)}$, at a Pb/diamond interface taking into account contributions from elastic scattering, $\sigma_K^{(2)}$(DMM), inelastic three phonon scattering, $\sigma_K^{(3)}$, and inelastic four phonon scattering, $\sigma_K^{(4)}$. The contributions from each of the elastic and inelastic scattering processes to σ_K are also shown in addition to Pb/H/diamond data from Lyeo and Cahill (Ref. 7). Taking into account three and four phonon process in thermal boundary conductance calculations shows excellent agreement to the experimental data, a significant improvement compared to predictions with the DMM assuming elastic scattering, $\sigma_K^{(2)}$(DMM).

$\times(\omega,T)$. Therefore, taking into account multiple phonon inelastic scattering, thermal boundary conductance can be calculated by

$$\sigma_K=\frac{\partial}{\partial T}\left[\sum_j\int_{\omega_{c,1,j}}\pi I_{1,j}(\omega,v,T)\sum_{n=2}^{n_{\max}}\alpha_{12}^{(n)}d\omega\right], \tag{18}$$

or, assuming a Debye dispersion,

$$\sigma_K=\frac{\hbar^2}{8\pi^2k_BT^2}\sum_j\frac{1}{v_{1,j}^2}\int_{\omega_{c,1,j}}\omega^4\frac{\exp\left[\frac{\hbar\omega}{k_BT}\right]}{\left(\exp\left[\frac{\hbar\omega}{k_BT}\right]-1\right)^2}\times\sum_{n=2}^{n_{\max}}\alpha_{12}^{(n)}d\omega, \tag{19}$$

where $\alpha_{12}^{(2)}$ is calculated by Eq. (7) and $\alpha_{12}^{(n)}$ when $n>2$ is calculated by Eq. (17). Since the phonon intensities are additive, Eq. (19) can be recast as

$$\sigma_K=\sum_{n=2}^{n_{\max}}\sigma_K^{(n)}, \tag{20}$$

where $\sigma_K^{(n)}$ represents the thermal boundary conductance due to n phonon scattering processes. Note that Eq. (20) requires no fitting parameters, only knowledge of the phonon velocity and oscillator density in the two materials adjacent to the interface. Using Eq. (20), the contributions of two phonon (elastic), and three and four phonon (inelastic) processes to thermal boundary conductance are calculated and shown in Fig. 2 for a Pb/diamond interface. Also shown in Fig. 2 are σ_K measurements of Pb films on hydrogen-terminated diamond substrates (Pb/H/diamond).[7] Note that the effects of hydrogen termination could have reduced the amount of Pb/diamond mixing during deposition[38] and therefore potentially represent a "cleaner" more abrupt interface than nonhydrogen-terminated samples. This simplifies the theory since σ_K predictions do not have to incorporate a mixing region at the interface creating phonon attenuation.[19,20] The two phonon (elastic) calculation, $\sigma_K^{(2)}$, which is the traditionally used DMM, significantly underpredicts the data and predicts a constant σ_K above ~100 K (a Debye temperature of Pb ~105 K).[27] The three phonon process contribution to thermal boundary conductance, $\sigma_K^{(3)}$, continues to increase above the Debye temperature since the high frequency phonons in the diamond substrate that are participating in σ_K^3 are being quantum mechanically populated up to the Debye temperature of diamond (~2230 K).[27] A similar trend is observed in the four phonon process contribution to thermal boundary conductance, $\sigma_K^{(4)}$. The total predicted thermal boundary conductance shows excellent agreement in value and trend to the measured Pb/H/diamond thermal boundary conductance, indicating that multiple phonon inelastic scattering is being observed in the experimental data. Note that the contribution of $\sigma_K^{(4)}$ compared to the overall predicted thermal boundary conductance, $\sigma_K=\sigma_K^{(2)}+\sigma_K^{(3)}+\sigma_K^{(4)}$, is less than 10% at the temperatures of interest. Therefore, three phonon processes are dominating thermal boundary conductance. This was qualitatively inferred by Hopkins *et al.*[6] and Lyeo and Cahill.[7] Due to the relatively low contribution of four phonon processes to the overall σ_K, higher order phonon processes are not considered in the remainder of this analysis since the contribution of these processes are less than that of $\sigma_K^{(4)}$.

Figure 3 shows the same calculations as Fig. 2 for Bi/H/diamond, Au/diamond, Pt/Al_2O_3, and Pt/AlN interfaces. Again, taking into account three and four phonon processes in Bi/diamond and Au/diamond give much better agreement in values and trends of the predicted σ_K. These two samples are heavily mismatched, and the calculations of the elastic

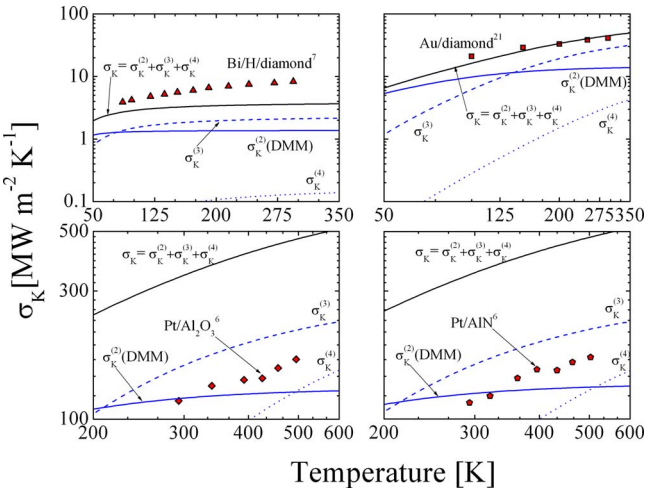

FIG. 3. (Color online) The total predicted thermal boundary conductance, $\sigma_K=\sigma_K^{(2)}+\sigma_K^{(3)}+\sigma_K^{(4)}$, at four different interfaces taking into account contributions from elastic scattering, σ_K^2(DMM), inelastic three phonon scattering, $\sigma_K^{(3)}$, and inelastic four phonon scattering, $\sigma_K^{(4)}$. The contributions from each of the elastic and inelastic scattering processes to σ_K are also shown in addition to Bi/H/diamond data from Lyeo and Cahill (Ref. 7), Au/diamond data from Stoner and Maris (Ref. 21), and Pt/Al_2O_3 and Pt/AlN data from Hopkins *et al.* (Ref. 6). The Debye temperatures of Bi, Au, Pt, Al_2O_3, and AlN are 119 (Ref. 27), 165 (Ref. 27), 240 (Ref. 27), 1043 (Ref. 40), and 1150 K (Ref. 41), respectively.

transmission coefficient calculated with the DMM gives a good estimation of the elastic scattering contribution.[33] However, as the samples become less heavily mismatched (i.e., more acoustically similar), the assumptions governing the elastic transmission coefficient fail. In the Pt samples, taking into account three and four phonon processes causes an overprediction of the calculations compared to the data. Note, however, that the trend in inelastic total thermal boundary conductance matches that of the experimental data. Remember, the increasing trend of σ_K above one materials' Debye temperature is the original evidence of inelastic scattering from MDS.[25,26] All of the predictions of σ_K using three or three and four phonon processes capture this trend. For example, the slope of the Pt/Al_2O_3 data is 0.22 MW m^{-2} K^{-2} over 300–500 K. Over this temperature range, the DMM predicts a slope of about 0.03 MW m^{-2} K^{-2}, which is about ten times lower than the experimentally measured slope. However, the model taking into account three and four phonon processes predict a slope of 0.63 MW m^{-2} K^{-2}, which is of the same order of magnitude (about three times larger) as the slope observed in the experiments, thus quantifying the improvement in σ_K predictions that take into account inelastic processes over the DMM predictions. This improvement is more obvious in the more heavily mismatched samples shown in Figs. 2 and 3.

The model developed in this paper takes into account a high frequency phonon breaking down into multiple lower frequency phonons of the same frequency. Although phonons are not required to break down into multiple phonons of the same frequency, this assumption allows for the development of a closed form, analytical model taking into account inelastic scattering at solid interfaces. High level computer simulations such as molecular dynamics and wave packet analyses can elucidate more physics into multiple phonon interfacial processes.[26,39] In addition, this model assumes that if there is energy for a multiple phonon process to occur, then it will occur. However, the interfacial scattering probabilities have never been studied, and without probabilistic simulations such as Monte Carlo or specific experimental data on phonon lifetimes at interfaces, there is no way to know what specific interfacial phonon events are allowed or not allowed.

In conclusion, a new model is developed that accounts for inelastic scattering in thermal boundary conductance. By taking into account conservation of energy and phonon population, the decay of a high frequency phonon into several lower frequency phonons can be specifically modeled, and assuming diffuse scattering at the interface, the transmission probability can be explicitly calculated. Using this new form of transmission probability that takes into account inelastic phonon scattering processes at the interface, better agreement in values and trends between thermal boundary conductance calculations and experimental data is observed as opposed to the agreement observed between traditional DMM calculations that only assume elastic scattering. The power of this new model lies in the fact that there are no fitting parameters, all that is necessary for prediction of the various inelastic phonon scattering events is knowledge of the phonon velocity and oscillator density in both materials. This model and the analysis in this paper show that inelastic phonon scattering dominates thermal boundary conductance in acoustically mismatched samples, with the most significant contribution coming from three phonon process.

ACKNOWLEDGMENTS

The author is greatly appreciative for funding by the Harry S. Truman Fellowship Program at Sandia National Laboratories. Sandia is a multiprogram laboratory operated by Sandia Corporation, a Lockheed-Martin Co., for the U.S. Department of Energy's National Nuclear Security Administration under Contract No. DE-AC04-94AL85000.

[1] P. L. Kapitza, Zh. Eksp. Teor. Fiz. Pis'ma Red. **11**, 1 (1941).
[2] R. S. Prasher, Phys. Rev. B **77**, 075424 (2008).
[3] S.-M. Lee, D. G. Cahill, and R. Venkatasubramanian, Appl. Phys. Lett. **70**, 2957 (1997).
[4] D. Li, Y. Wu, R. Fan, P. Yang, and A. Majumdar, Appl. Phys. Lett. **83**, 3186 (2003).
[5] B. C. Gundrum, D. G. Cahill, and R. S. Averback, Phys. Rev. B **72**, 245426 (2005).
[6] P. E. Hopkins, R. J. Stevens, and P. M. Norris, ASME J. Heat Transfer **130**, 022401 (2008).
[7] H.-K. Lyeo and D. G. Cahill, Phys. Rev. B **73**, 144301 (2006).
[8] D. G. Cahill, W. K. Ford, K. E. Goodson, G. D. Mahan, A. Majumdar, H. J. Maris, R. Merlin, and S. R. Phillpot, J. Appl. Phys. **93**, 793 (2003).
[9] C. W. Chang, D. Okawa, H. Garcia, A. Majumdar, and A. Zettl, Phys. Rev. Lett. **101**, 075903 (2008).
[10] E. T. Swartz and R. O. Pohl, Appl. Phys. Lett. **51**, 2200 (1987).
[11] R. M. Costescu, M. A. Wall, and D. G. Cahill, Phys. Rev. B **67**, 054302 (2003).
[12] Y. K. Koh and D. G. Cahill, Phys. Rev. B **76**, 075207 (2007).
[13] P. E. Hopkins, P. M. Norris, R. J. Stevens, T. Beechem, and S. Graham, ASME J. Heat Transfer **130**, 062402 (2008).
[14] R. J. Stevens, A. N. Smith, and P. M. Norris, ASME J. Heat Transfer **127**, 315 (2005).
[15] E. T. Swartz and R. O. Pohl, Rev. Mod. Phys. **61**, 605 (1989).
[16] P. E. Phelan, ASME J. Heat Transfer **120**, 37 (1998).
[17] P. Reddy, K. Castelino, and A. Majumdar, Appl. Phys. Lett. **87**, 211908 (2005).

[18]A. Majumdar and P. Reddy, Appl. Phys. Lett. **84**, 4768 (2004).
[19]T. E. Beechem, S. Graham, P. E. Hopkins, and P. M. Norris, Appl. Phys. Lett. **90**, 054104 (2007).
[20]R. S. Prasher and P. E. Phelan, ASME J. Heat Transfer **123**, 105 (2001).
[21]R. J. Stoner and H. J. Maris, Phys. Rev. B **48**, 16373 (1993).
[22]M. L. Huberman and A. W. Overhauser, Phys. Rev. B **50**, 2865 (1994).
[23]A. V. Sergeev, Phys. Rev. B **58**, R10199 (1998).
[24]A. V. Sergeev, Physica B **263–264**, 217 (1999).
[25]Y. Chen, D. Li, J. Yang, Y. Wu, J. Lukes, and A. Majumdar, Physica B **349**, 270 (2004).
[26]R. J. Stevens, L. V. Zhigilei, and P. M. Norris, Int. J. Heat Mass Transfer **50**, 3977 (2007).
[27]C. Kittel, *Introduction to Solid State Physics*, 7th ed. (Wiley, New York, 1996).
[28]P. G. Klemens, Phys. Rev. **148**, 845 (1966).
[29]G. Chen, Phys. Rev. B **57**, 14958 (1998).
[30]C. Dames and G. Chen, J. Appl. Phys. **95**, 682 (2004).
[31]P. E. Hopkins and P. M. Norris, Nanoscale Microscale Thermophys. Eng. **11**, 247 (2007).
[32]Y. A. Kosevich, Phys. Rev. B **52**, 1017 (1995).
[33]P. E. Hopkins and P. M. Norris, J. Heat Transfer **131**, 022402 (2009).
[34]G. Chen, *Nanoscale Energy Transport and Conversion: A Parallel Treatment of Electrons, Molecules, Phonons, and Photons* (Oxford University Press, New York, 2005).
[35]Z. Zhang, *Nano/Microscale Heat Transfer* (McGraw-Hill, New York, 2007).
[36]D. E. Gray, *American Institute of Physics Handbook*, 3rd ed. (McGraw-Hill, New York, 1972).
[37]M. Balkanski, R. F. Wallis, and E. Haro, Phys. Rev. B **28**, 1928 (1983).
[38]K. Oura, V. G. Lifshits, A. A. Saranin, A. V. Zotov, and M. Katayama, Surf. Sci. Rep. **35**, 1 (1999).
[39]P. K. Schelling, S. R. Phillpot, and P. Keblinski, Appl. Phys. Lett. **80**, 2484 (2002).
[40]R. Q. Fugate and C. A. Swenson, J. Appl. Phys. **40**, 3034 (1969).
[41]M. E. Levinshtein, S. L. Rumyantsev, and M. S. Shur, *Properties of Advanced Semiconductor Materials: GaN, AlN, InN, BN, SiC, SiGe* (Wiley-Interscience, New York, 2001).